Available online at www.sciencedirect.com
SCIENCE DIRECT®
Journal of Colloid and Interface Science 257 (2003) 357–363
JOURNAL OF Colloid and Interface Science
www.elsevier.com/locate/jcis

Spontaneous detachment of oil drops from solid substrates: governing factors

V.L. Kolev,[a] I.I. Kochijashky,[a] K.D. Danov,[a] P.A. Kralchevsky,[a,*]
G. Broze,[b] and A. Mehreteab[c]

[a] *Laboratory of Chemical Physics & Engineering, Faculty of Chemistry, University of Sofia, 1164 Sofia, Bulgaria*
[b] *Colgate–Palmolive R&D, Inc., Avenue du Parc Industriel, B-4041 Milmort (Herstal), Belgium*
[c] *Colgate–Palmolive Technology Center, Piscataway, NJ 08854-5596, USA*

Received 24 May 2002; accepted 22 October 2002

Abstract

We carried out experiments on detachment of oil drops from glass substrates in solutions of an anionic surfactant. The three-phase contact line shrinks spontaneously, and eventually the oil drop detaches from the substrate. Consecutive video frames of such drops are digitized, and the time dependencies of the contact radius and angle are determined. Three stages of detachment of a drop, situated above a horizontal substrate, can be distinguished. They correspond to three different driving factors: (1) the interfacial tension decrease because of surfactant adsorption, (2) the aqueous meniscus spontaneously advances owing to the penetration of water between the oil and solid phases, and (3) at sufficiently small contact radius the shape of the oil–water interface becomes unstable and the drop detaches under the action of buoyancy. Analyzing the experimental data, we identified two important characteristics of the drop-detachment process: the velocity of spontaneous advance of the contact line and the line drag coefficient. In the case of moving contact line, a dynamic Young equation must be used, which takes into account the line drag force. The latter is proportional to the velocity of contact-line motion. The experimental data agree with the latter dependence, from whose slope the line drag coefficient is determined.

Keywords: Cleaning of oil from solid surface; Contact angle; Detachment of oil drops from solid substrate; Detergency; Drag force at moving contact line; Dynamic contact line; Roll-up mechanism; Young equation—dynamic

1. Introduction

Several mechanisms have been discussed in the literature in relation to the cleaning of solid surfaces from oily deposits. The most popular are roll-up, emulsification, and solubilization [1–10]. Depending on the specific system, one or another mechanism can prevail. From a practical viewpoint it is important to reveal the physicochemical factors that can be used for efficient control of the cleaning process. One of these factors is the type and concentration of the surfactants used. The latter can affect the cleaning process by changing the oil–water and solid–water interfacial tensions, the three-phase contact angle, the solubility of the oil in the aqueous phase, etc. Important details of the washing action of surfactant solutions are not yet well understood, because the actual process is rather complex and could combine two or several elementary mechanisms.

Our present study is directed toward analyzing the mechanism of spontaneous detachment of oil drops from solid surfaces in solutions of ionic surfactants. We carried out direct microscopic observations of the cleaning process for hydrophilic glass surfaces, in an attempt to reveal the main stages of the oil drop detachment. The final goal is to get additional knowledge about the main factors that control the cleaning process and can be used for its optimization.

Technologically oriented experiments on detachment of oil drops from solid substrates were carried out by Dillan et al. [3], who obtained many data about the efficiency of the roll-up mechanism. The experiments of several authors [6,11–13] show that the apparent "roll-up" is related to shrinking of the three-phase solid–oil–water contact line, which, in its turn, is due to the molecular penetration (diffusion) of water molecules between the oil drop and the solid phase. This process was termed the *diffusional* mechanism

* Corresponding author.
E-mail address: pk@lcpe.uni-sofia.bg (P.A. Kralchevsky).

0021-9797/03/$ – see front matter
PII: S0021-9797(02)00052-8

of oil detachment. For example, in the experiments by Kao et al. [6], drops of crude oil have been detached from glass in solutions of 1 wt% C_{16}-alpha-olefin-sulfonate + 1 wt% NaCl. These authors have observed directly the dynamics of water-film penetration between the oil phase and the solid. Once such a disjoining water film has been formed, even a weak shear flow is enough to detach the oil drop from the substrate. The study in Ref. [6] was related to enhanced oil recovery; however, a similar mechanism can be operative also for oil-drop detachment in other applications of detergency. To our best knowledge, the physicochemical and dynamic aspects of the *diffusional* mechanism have not yet been well studied and understood.

From a more general viewpoint, processes with moving contact lines are crucial for many applications in coating, printing, painting, and detergency. The most studied are the cases where the motion of the contact line on a solid surface is strained by some external force or potential gradient, including processes of liquid deposition on a moving or porous substrate; see Refs. [14–28] and the literature cited therein. In contrast, in the case of a diffusional mechanism [6], the contact-line motion occurs spontaneously, at a finite contact angle, driven by some molecular mechanisms, but its velocity is much lower than in the case of conventional spreading (zero contact angle; see, e.g., Ref. [29]) or "superspreading" [30].

Our aim here is to investigate the *dynamic* aspects of the diffusional mechanism of detachment of oil drops from a horizontal glass plate immersed in a surfactant solution. Our attention is focussed on the balance of forces at the moving three-phase contact line. In such cases, a *line drag force* should be included in the Neumann–Young force balance at the contact line [31]. One of our goals is to verify this expectation and to determine the *line drag coefficient*. The latter could be an important physicochemical parameter characterizing the dynamics of detachment of oil drops.

The paper is organized as follows. In Section 2 we describe the experimental method. Section 3 is devoted to the procedure of processing of the drop profiles. Section 4 presents the results and their interpretation.

2. Experimental method and procedures

In our experiments we use the same *surfactant* as in Ref. [6], C_{14}/C_{16}-alfa-olefin-sulfulate (AOS) sodium salt, technical product, Hostapur OSB (Clariant). The working AOS concentration was from 0.3 to 1 mM. The solutions also contained various concentrations of NaCl (Merck, analytical grade, preheated for 5 h at 450 °C) in deionized water from a Milli-Q Organex purification system. Pure hexadecane was used as the oil phase.

Dry glass slides, precleaned by immersion in sulfochromic acid and subsequent abundant rinsing with water, were used as substrates. After the rinsing, the glass slides were dried at 80 °C for 1 h. In our experiments, a hexadecane drop of millimeter size is placed on the *dry* glass slide. Then, the slide is placed (with the oil drop at the upper side) at the horizontal bottom of the experimental rectangular glass vessel, which has planar walls to prevent optical distortion. Afterwards, the surfactant solution is carefully poured into the vessel until completely immersing the oil drop in the solution. Furthermore, by using a horizontal microscope with a long-focus objective, one can observe the drop profile. A digital CCD camera (Kappa CF 8/1 DX) and VCR (Samsung SV-4000) were used to record the process of drop detachment. All experiments were carried out at the ambient room temperature ($T = 22 \pm 2\,^{\circ}\mathrm{C}$).

Consecutive experimental photos of a drop, at different stages of spontaneous detachment, are shown in Fig. 1 (0.3 mM AOS + 100 mM NaCl). It is visible that initially the drop has an approximately spherical shape. With elapsed time the contact line shrinks, the oil–solid contact area decreases, and the drop becomes slightly elongated under the action of buoyancy (pendant-drop-type profile). At the final stage ($t = 878$ s) a neck is formed. Next, the drop detaches very fast. Depending on the surfactant concentration and the volume of the deposited drop, sometimes a residual drop is observed to remain on the substrate; that is, the initial drop has broken at the neck. In other cases, complete oil detachment, without residual drop, is observed.

Video frames of the drop were digitized and recorded. The data for each digitized drop profile were processed numerically to adjust the cap of the drop at the center of the coordinate system and to rotate the profile in order to get the vertical axis coincident with the axis of symmetry. This computational procedure is important for the following two reasons: (a) the original image is digitized in the real screen frame, i.e., in a shifted coordinate system; (b) the original image is sometimes taken rotated at a small angle with respect to the vertical due to imperfect positioning of the video camera. Digitized profiles of the drop in Fig. 1 are shown in Fig. 2, where the drop dimensions are quantified.

We measured the water/hexadecane interfacial tension by the spinning drop method (Krüss). The measured equilibrium interfacial tension of 0.3 mM AOS + 0.1 M NaCl is 3.9 mN/m.

3. Processing of the drop profiles

To achieve an accurate determination of the radius of the three-phase contact line, r_c, and the contact angle, α, we fitted the obtained digital drop profiles (Fig. 2) by means of the Laplace equation of capillarity. The physical parameters involved in the Laplace equation are the capillary pressure and the characteristic capillary length,

$$l = \left[(\rho_{\mathrm{w}} - \rho_{\mathrm{o}})g/\sigma_{\mathrm{ow}}\right]^{-1/2}, \tag{1}$$

where σ_{ow} is the oil–water interfacial tension, g is the acceleration due to gravity, and $\rho_{\mathrm{w}} = 0.998$ g/cm^3 and

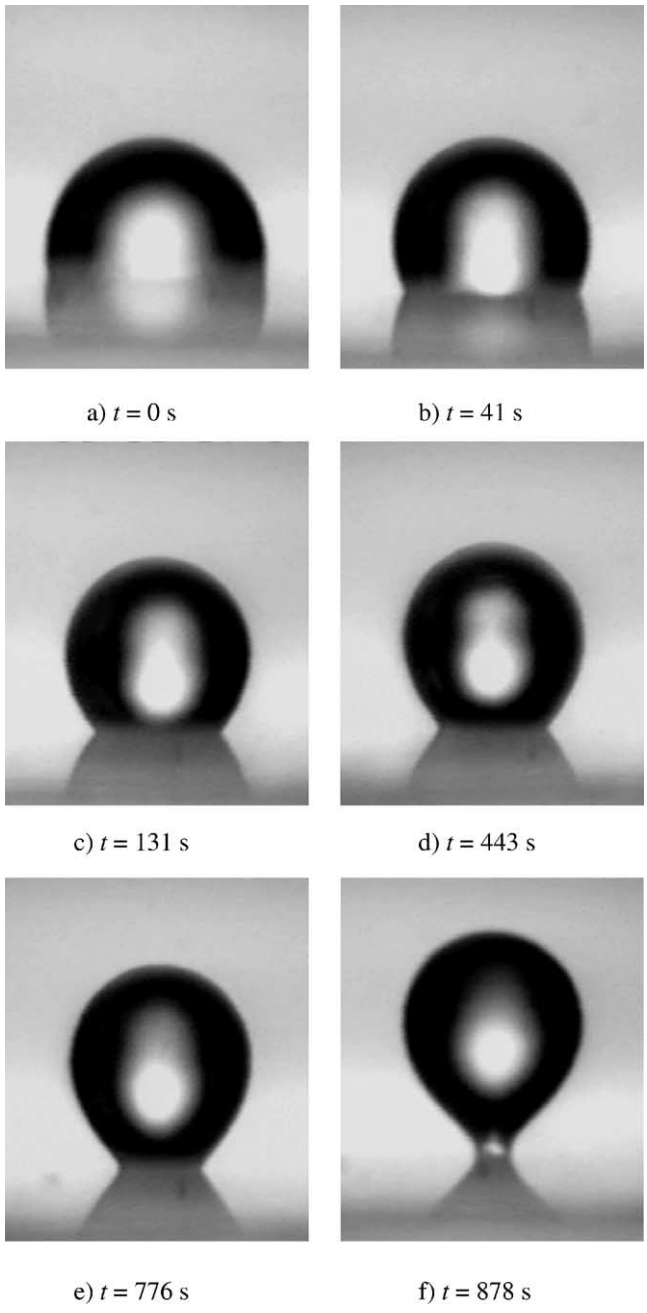

Fig. 1. Consecutive photos of the process of detachment of a hexadecane drop from a horizontal glass plate immersed in a solution of 0.3 mM AOS + 0.1 M NaCl.

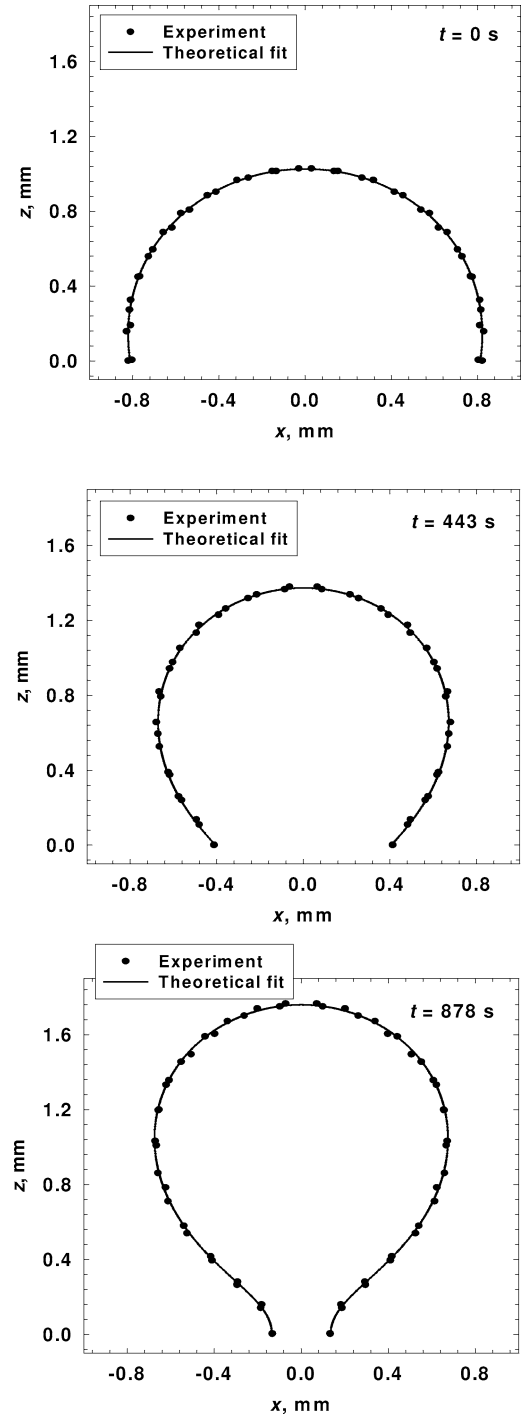

Fig. 2. Digitized profiles of three of the photos in Fig. 1 taken at time moments denoted in the figure. The theoretical line is drawn as explained in Section 3.

$\rho_o = 0.772$ g/cm^3 are the densities of water and hexadecane at 22 °C.

A cylindrical coordinate system, *Orz*, is used, with r and z being the radial and vertical coordinates, respectively. It is convenient to chose the coordinate origin at the drop apex and to orient the z-axis downward (Fig. 3). We introduce dimensionless variables

$$x_1 = \frac{r}{l}, \qquad x_2 = \frac{z}{l}, \qquad v = \frac{V}{\pi l^3}, \tag{2}$$

where V is the volume of the drop, which remains constant during the detachment experiment (no solubilization of oil).

For the sake of numerical integration, it is convenient to represent the Laplace equation of capillarity in terms of the arc length, s, along the generatrix of the drop profile [32],

$$\frac{d\theta}{ds} = \frac{2}{b} - \frac{\sin\theta}{x_1} - x_2, \qquad \frac{dx_1}{ds} = \cos\theta, \qquad \frac{dx_2}{ds} = \sin\theta, \tag{3}$$

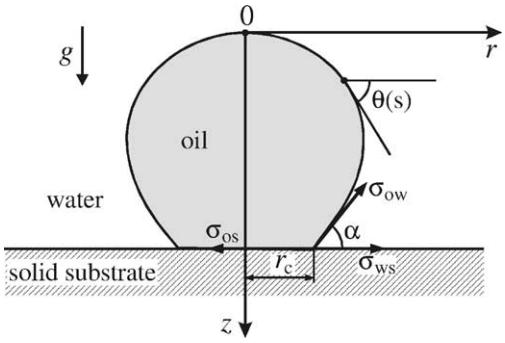

Fig. 3. Sketch of an oil drop situated above a horizontal solid plate immersed in a water phase. The interfacial tensions, σ_{ow}, σ_{os}, and σ_{ws}, acting at the three-phase contact line (of radius r_c) are shown; α is the contact angle; θ is running slope angle; g is the acceleration due to gravity.

where $\theta = \theta(s)$ is the running slope angle and b is the unknown dimensionless radius of curvature at the top of the drop (Fig. 3). Thus, the Laplace equation acquires the form of a system of three differential equations which is solved to determine the functions $x_1 = x_1(s)$, $x_2 = x_2(s)$, and $\theta = \theta(s)$ describing the drop profile in a parametric form. To find the solution of Eq. (3), three natural boundary conditions are used at the drop apex, where s is defined to be zero:

$$x_1(0) = 0, \qquad x_2(0) = 0, \qquad \theta(0) = 0. \tag{4}$$

Equation (4) determines the starting point for the numerical integration along the drop profile.

Three parameters enter the set of equations: (i) the interfacial tension, σ_{ow}, which defines the capillary length, l; (ii) the drop volume, V, which is constant; and (iii) the radius of curvature at the drop apex, b. First, we fit carefully the profile of the initial drop, at $t = 0$, which has an almost spherical shape, and determine the drop volume. For example, for the drop in Figs. 1 and 2 we get $V = 1.45\ \text{mm}^3$. Afterwards, we keep V constant and fit all other profiles only with two unknown parameters, b and σ_{ow}. The fit is excellent; it describes well the drop shapes in the cases with and without neck (see Fig. 2). From the best fits we calculate the contact radius r_c, the contact angle, α, and the interfacial tension, σ_{ow}. The last is found to vary with time due to simultaneous surfactant adsorption and deformation of the drop shape.

4. Numerical results and discussion

Figure 4 shows the results from the processing of 24 consecutive experimental profiles of one and the same detaching oil drop. The results for the contact radius r_c and contact angle, α, are shown in Fig. 4 as functions of time t. During the first 160 s (Stage I) r_c quickly decreases, from 0.81 mm to 0.50 mm. Afterwards, r_c decreases slowly, from 0.50 mm to 0.30 mm, for a long period of about 620 s (Stage II). The final Stage III of drop detachment is very fast: r_c shrinks down to 0.12 mm, a capillary instability of the drop profile appears, and the drop detaches (see Fig. 4a).

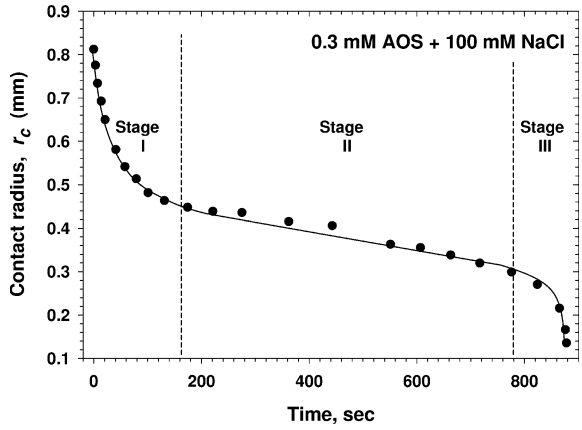

(a)

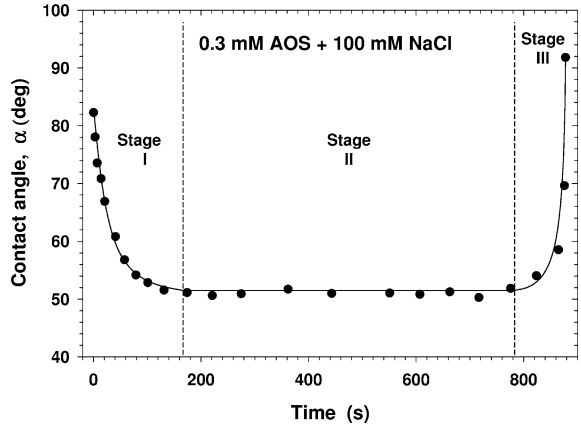

(b)

Fig. 4. (a) Contact radius r_c and (b) contact angle α as functions of time t. The points are obtained by processing digitized photos of the drop in Fig. 1; the lines are guides to the eye.

The contact angle (Fig. 4b) also shows three stages with different behavior. Initially, during Stage I, the contact angle α drops from 83° down to 50°. During Stage II α does not change significantly—it remains constant, about 50°. In the final Stage III, α increases fast up to 92°. The points in Figs. 5a and 5b form almost smooth lines (no scattering); that is, the experimental errors are low.

The dependencies $r_c(t)$ and $\alpha(t)$ can be interpreted in the following way. During all stages, there is a dynamic balance of forces per unit length of the contact line, which reads

$$\sigma_{os} = \sigma_{ws} + \sigma_{ow}\cos\alpha + \sigma_d. \tag{5}$$

Here σ_{os} and σ_{ws} are the superficial tensions of the oil–solid and water–solid boundaries (Fig. 3); σ_d is a drag force acting per unit length of the contact line; σ_d is expected to be proportional to the velocity of motion of the contact line,

$$\sigma_d = -\beta\frac{dr_c}{dt}, \tag{6}$$

where β is a *line* drag coefficient. (Note that σ_d is positive because dr_c/dt is negative; in general, σ_d is directed oppositely to the direction of contact-line motion). Equation (6)

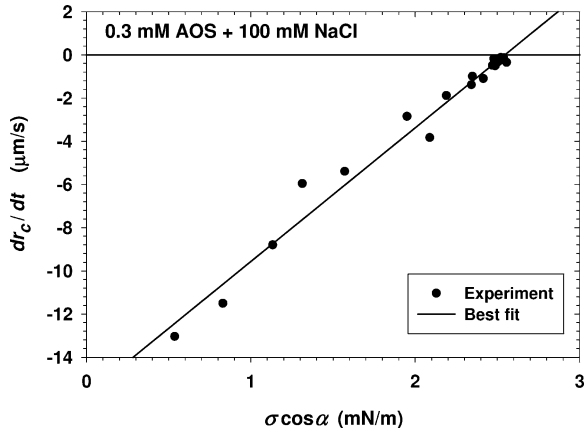

Fig. 5. Experimental velocity of motion of the contact line, dr_c/dt, plotted vs $\sigma\cos\alpha$ in accordance with Eq. (9).

can be deduced from Eq. (40) in Ref. [31], which expresses the balance of the thermodynamic force by the drag force at steady state conditions.

It should be noted that the Young equation can be derived based on both energy and force considerations, the two approaches being equivalent. In particular, the force interpretation of σ_{os} and σ_{ws} stems from the work of Gibbs [33], who coined the term "superficial tensions" for them. According to Gibbs [33], by definition, the superficial tension opposes every increase of the wet area, without any deformation of the solid, in the same way as σ_{ow} opposes every dilatation of the interface between the two fluids. From this viewpoint, the superficial tensions σ_{os} and σ_{ws} can be interpreted as surface tensions, i.e., *forces* per unit length. Thus, the Young equation has the meaning of a tangential projection of a vectorial force balance per unit length of the contact line. Correspondingly, the normal component of the meniscus surface tension, $\sigma_{ow}\sin\alpha$ (Fig. 3), is counterbalanced by the bearing reaction of the solid substrate.

In fact, Eq. (5) represents a dynamic form of the Young equation with account for the viscous drag force. The physical reason for the appearance of line drag force is the fact that (during the motion of the contact line) oil molecules are taken out of potential wells at the solid surface and replaced by water molecules, accompanied with dissipation of kinetic energy in the zone of the contact line. In particular, a possible interpretation of the three stages distinguished in Fig. 4 is the following.

Stage I. In the beginning, the interfacial tension σ_{ow} quickly decreases due to the adsorption of surfactant at the oil–water interface. The lowering of σ_{ow} affects the force balance at the three-phase contact line. The latter shrinks to reach an equilibrium position, with an appropriate value of the contact angle. In other words, during Stage I the variation of σ_{ow} is the driving force of the observed contact-line shrinking.

Stage II. In this stage σ_{ow} and α have already reached their almost equilibrium values, $\sigma_{ow,eq} \approx 3.9$ dyn/cm and $\alpha_{eq} \approx 50°$. Because at this stage the rate of motion of the contact line, dr_c/dt, is rather small, one can neglect σ_d in Eq. (5) (an estimate is given below) to obtain

$$\sigma_{os} = \sigma_{ws} + \sigma_{eq}\cos\alpha_{eq} \quad \text{(Stage II)}. \tag{7}$$

Figure 4a shows that the contact line still shrinks very slowly. The slope of the curve in Fig. 4a, corresponding to the intermediate Stage II, is

$$u_s = |dr_c/dt|_{\text{Stage II}} = 0.24\ \mu\text{m/s}. \tag{8}$$

In fact, u_s has the meaning of the velocity of spontaneous motion of the contact line. This could be attributed to the molecular diffusion of water (and surfactant?) along the oil–solid boundary in the zone of the three-phase contact. The diffusion of water disjoins the oil from the solid at the contact line. Such a process could be the origin of the slow changes during Stage II. We believe that u_s is an important kinetic characteristic of the oil–drop detachment. Its dependence on the composition of the surfactant solution, type of oil and solid, size of the drop, etc., should be investigated.

Stage III. This stage begins when the contact line radius r_c becomes so small that the shape of the pendant oil drop becomes unstable. This type of instability ("necking") has been investigated in relation to the drop-volume method for measurement of surface tension [34–39]. The necking develops at a finite rate because of the viscous dissipation of kinetic energy in the oil and water phases, and in the contact-line region.

Note that Eq. (5) is satisfied during all three stages of drop detachment. This equation implies that under steady-state conditions the disbalance of the interfacial tensions at the contact line is always counterbalanced by the *line drag force*, σ_d, by adjustment of a corresponding velocity of the contact-line motion, dr_c/dt. Substituting Eqs. (6) and (7) into Eq. (5), we obtain

$$\frac{dr_c}{dt} = \frac{1}{\beta}(\sigma\cos\alpha - \sigma_{eq}\cos\alpha_{eq}). \tag{9}$$

In accordance with Eq. (9), in Fig. 5 we plot the experimental data for dr_c/dt vs. $\sigma\cos\alpha$ for all the three stages. The data comply well with a straight line, which confirms the validity of Eq. (6). Note that the experimental points on the right-hand side of Fig. 5 correspond to the intermediate Stage II, whereas the points on the left correspond to the more dynamic initial and final Stages I and III.

From the slope of the linear regression (Fig. 5) we determine the line drag coefficient to be $\beta = 16.2$ poise (1.62 Pa s). The intercept yields $\sigma_{eq}\cos\alpha_{eq} = 2.55$ mN/m; with $\alpha_{eq} \approx 50°$ this yields $\sigma_{eq} = 3.95$ mN/m, in agreement with the spinning-drop measurements. Using Eq. (8), one obtains that during Stage II the line drag is $\sigma_d = \beta u_s = 3.9 \times 10^{-4}$ dyn/cm. In other words, σ_d is really negligible during Stage II, for which the equilibrium relation, Eq. (7), holds.

Next, let us discuss the difference between the detachment in the case of oil drops situated below (Ref. [6]) and above (the present article) the solid substrate. In the latter case, the buoyancy force tends to detach the drop from the substrate; for that reason, when water penetrates between oil and glass in the contact zone, the oil and glass surfaces readily detach, and a continuous shrinking of the contact line (advancing of the water meniscus) is observed. In contrast, in the case of oil drop below a glass plate, the buoyancy pushes the drop toward the solid surface. Then, during Stage II, the penetration of water between oil and glass in the contact zone leads to the formation of water lenses, rather than to advancing of the water meniscus [6].

The reproducibility of the experimental data, such as those in Fig. 4, is sensitive to the pretreatment of the solid surface. The experiments carried out with different drops and glass plates give qualitatively similar results, although there are often quantitative differences. The latter could be due, at least in part, to the differences between the initial volumes of the drops. Tasks for future studies can be to determine whether and how the velocity of spontaneous contact-line advance, u_s, and the line drag coefficient, β, depend on the drop volume, type of surfactant, surfactant concentration and micellization, presence of added inorganic electrolytes (hardness of water), type of oil, chemical nature and surface roughness of the solid substrate; effect of applied cross flow in the water phase, etc.

Finally, let us discuss a possible mechanism of penetration of the oil–glass interface by water as the likely cause of the continuing detachment process. There are many experimental indications that water may dissolve or diffuse into and swell the glass (and silica) surface and form a surface gel layer [40–48]. This effect shows up in surface-force measurements [44,46,48] and in experiments on adsorption of macromolecules on glass [47]. As part of the dissolution process, water may break silicon–oxygen bonds and form a hydroxylated surface [48]. In addition, the formation of a gel layer may include an ion exchange process, in which sodium ions at the glass surface are replaced by protons [41,43,47]. Swelling of the surface layers has been directly detected in some glasses in humid atmospheres by analytical methods: the surface area is increased by at least 10 times, micropores appear, and clusters are formed on the interface [45]. Coming back to our system (Fig. 3), we could hypothesize that water molecules, from the gel layer at the water–glass interface, can penetrate the oil–water interface by diffusion, at least in the close vicinity of the contact line. The presence of water molecules in the surface layer of glass would alter the values of the two superficial tensions, σ_{ws} and σ_{os}, which, in turns, would affect the force balance expressed by the dynamic Young equation, Eq. (5). The resulting uncompensated force would drive the spontaneous shrinking of the contact line. A model development is under way.

5. Summary and conclusions

We carried out experiments on detachment of oil drops from glass substrates in solutions of the ionic surfactant AOS. Video frames of detaching oil drops were digitized (Fig. 1) and processed by means of the Laplace equation (Fig. 2), and the time dependencies $r_c(t)$ and $\alpha(t)$ were determined (Fig. 4).

One can identify the following stages of detachment of a drop situated above a horizontal substrate: Stage I (fast): the reason for the changes in the drop shape is the decrease of the interfacial tension due to surfactant adsorption. Stage II (slow): the changes in the drop shape are due to the spontaneous advance of the aqueous meniscus, with a constant velocity u_s, owing to the penetration of water between the oil and solid phases in the zone of the contact line. In our experiment $u_s = 240$ nm/s. Stage III (fast): this begins when r_c becomes so small that the shape of the oil–water interface becomes unstable and a "necking" instability appears; the driving force of the changes at this stage is the buoyancy.

Analyzing the experimental data we identified two important characteristics of the process of drop detachment, whose role deserves to be studied better in the future. These are (i) the velocity of spontaneous advance of the contact line (of the aqueous meniscus), u_s, and (ii) the line drag coefficient, β. In the case of a moving contact line a dynamic Young equation must be used, Eq. (5). It states that if there is a disbalance of the interfacial tensions at the contact line, the excess tension is counterbalanced by the line drag force, σ_d, which is proportional to the velocity of contact-line motion; see Eq. (6). The experimental data agree with Eq. (9), which is a form of the dynamic Young equation. From the slope of the respective linear regression (Fig. 5) we determined the line drag coefficient for this specific system ($\beta = 1.62$ Pa s).

Acknowledgment

This work was supported by Colgate–Palmolive.

References

[1] W.G. Cutler, R.C. Davis (Eds.), Detergency: Theory and Test Methods, Parts I–III, Dekker, New York, 1981.
[2] W.G. Cutler, E. Kissa (Eds.), Detergency: Theory and Technology, Dekker, New York, 1987.
[3] K.W. Dillan, E.D. Goddard, D.A. McKenzie, J. Am. Oil. Chem. Soc. 56 (1979) 59.
[4] M.C. Gum, E.D. Goddard, J. Am. Oil. Chem. Soc. 59 (1982) 142.
[5] M. Mahé, M. Vignes-Adler, A. Rosseau, C.G. Jacquin, P.M. Adler, J. Colloid Interface Sci. 126 (1988) 314.
[6] R.L. Kao, D.T. Wasan, A.D. Nikolov, D.A. Edwards, Colloids Surf. 34 (1988/1989) 389.
[7] B. Carroll, Colloids Surf. A 74 (1993) 131.
[8] C.A. Miller, K.H. Raney, Colloids Surf. 74 (1993) 169.
[9] L. Thompson, J. Colloid Interface Sci. 163 (1994) 61.

[10] P.A. Kralchevsky, K. Nagayama, Particles at Fluid Interfaces and Membranes, Elsevier, Amsterdam, 2001, p. 268.
[11] J. Powney, J. Text. Inst. Trans. 40 (1949) 549.
[12] D.G. Stevenson, J. Text. Inst. Trans. 42 (1951) 194.
[13] D.G. Stevenson, J. Text. Inst. Trans. 44 (1953) 548.
[14] V.E.B. Dussan, Ann. Rev. Fluid Mech. 11 (1979) 371.
[15] V.E.B. Dussan, E. Rame, S. Garoff, J. Fluid Mech. 137 (1983) 1.
[16] P.J. Haley, M.J. Miksis, Phys. Fluids A 3 (1991) 487.
[17] F. Brochard-Wyart, P.G. de Gennes, Adv. Colloid Interface Sci. 39 (1992) 1.
[18] Y.D. Shikhmurzaev, Int. J. Multiphase Flow 19 (1993) 589.
[19] E. Ruckenstein, J. Colloid Interface Sci. 170 (1995) 284.
[20] M.J. Savelski, S.A. Shetty, W.B. Kolb, R.L. Cerro, J. Colloid Interface Sci. 176 (1995) 117.
[21] A.W. Neumann, E. Rame, G. Garoff, Colloids Surf. A 116 (1996) 115.
[22] S.D. Iliev, J. Colloid Interface Sci. 213 (1999) 1.
[23] J.G. Petrov, J. Ralston, R.A. Hayes, Langmuir 15 (1999) 3365.
[24] R. Rame, J. Fluid Mech. 440 (2001) 205.
[25] R. Golestanian, E. Raphael, Phys. Rev. E 64 (2001) 031601.
[26] T.D. Blake, J. de Coninck, Adv. Colloid Interface Sci. 96 (2002) 21.
[27] C.N.C. Lam, R. Wu, D. Li, M.L. Hair, A.W. Neumann, Adv. Colloid Interface Sci. 96 (2002) 169.
[28] V.M. Starov, S.R. Kostvintsev, V.D. Sobolev, M.G. Velarde, S.A. Zhdanov, J. Colloid Interface Sci. 252 (2002) 397.
[29] A.W. Adamson, A.P. Gast, Physical Chemistry of Surfaces, 6th Ed., Wiley–Interscience, New York, 1997, Chapter IV.
[30] A.D. Nikolov, D.T. Wasan, A. Chengara, K. Koczo, G.A. Policello, I. Kolossvary, Adv. Colloid Interface Sci. 96 (2002) 325.
[31] P. Attard, Langmuir 16 (2000) 4455.
[32] S. Hartland, R. Hartley, Axisymmetric Fluid–Liquid Interfaces, Elsevier, Amsterdam, 1976.
[33] J.W. Gibbs, The Scientific Papers of J.W. Gibbs, Vol. 1, Dover, New York, 1961.
[34] T. Lohnstein, Ann. Phys. 20 (1906) 237;
T. Lohnstein, Ann. Phys. 20 (1906) 606;
T. Lohnstein, Ann. Phys. 21 (1906) 1030;
T. Lohnstein, Ann. Phys. 22 (1906) 767.
[35] W.D. Harkins, F.E. Brown, J. Am. Chem. Soc. 41 (1919) 499.
[36] B.B. Freud, W.D. Harkins, J. Phys. Chem. 33 (1929) 1217.
[37] E. Pitts, J. Inst. Math. Appl. 17 (1976) 387.
[38] R. Finn, Equilibrium Capillary Surfaces, Springer-Verlag, New York, 1986.
[39] D. Möbius, R. Miller (Eds.), Drops and Bubbles in Interfacial Research, Elsevier, Amsterdam, 1998.
[40] Th.F. Tadros, J. Lyklema, J. Electroanal. Chem. 17 (1968) 267.
[41] R.K. Iler, The Chemistry of Silica: Solubility, Polymerization, Colloid and Surface Properties and Biochemistry, Wiley, New York, 1979.
[42] R. Hunter, Foundation of Colloid Science, Clarendon, Oxford, 1987.
[43] R.H. Doremus, Glass Science, 2nd Ed., Wiley, New York, 1994.
[44] G. Vigil, Z. Xu, S. Steinberg, J.N. Israelachvili, J. Colloid Interface Sci. 165 (1994) 367.
[45] P. Trens, R. Denoyel, E. Guilloteau, Langmuir 12 (1996) 1245.
[46] V.V. Yaminsky, B.W. Ninham, R.M. Pashley, Langmuir 14 (1998) 3223.
[47] R.C. van Duijvenbode, G.J.M. Koper, M.R. Böhmer, Langmuir 16 (2000) 7713.
[48] J.J. Adler, Y.I. Rabinovich, B.M. Moudgil, J. Colloid Interface Sci. 237 (2001) 249.